

Research paper

# Scour formation due to simultaneous circular impinging jet and wall jet

MOJTABA MEHRAEIN, Post Doc. Researcher, *Tarbiat Modares University, Tehran, Iran, Visiting Researcher, Laboratory of Hydraulic Constructions (LCH), Ecole Polytechnique Fédérale de Lausanne (EPFL), Station 18, CH-1015 Lausanne, Switzerland.*  
Email: [mehraein@modares.ac.ir](mailto:mehraein@modares.ac.ir)

MASOUD GHODSIAN (IAHR Member), Professor, *Water Engineering Research Institute, Tarbiat Modares University, Tehran, Iran.*  
Email: [ghods@modares.ac.ir](mailto:ghods@modares.ac.ir) (author for correspondence)

ANTON J. SCHLEISS (IAHR Member), Professor, *Laboratory of Hydraulic Constructions (LCH), Ecole Polytechnique Fédérale de Lausanne (EPFL), Station 18, 1015 Lausanne, Switzerland.*  
Email: [anton.schleiss@epfl.ch](mailto:anton.schleiss@epfl.ch)

## ABSTRACT

Experiments involving both a circular wall jet and an impinging jet were conducted, as occurring at irrigation control structures or at dams with combined crest and low-level spillways. The effects of the non-dimensional parameters on the scour hole dimensions have been investigated. It was found that the effect of the expansion ratio of the channel width to the jet diameter is negligible for values larger than 22.5 and 35, depending on the experimental conditions. The scour depth decreases with increasing tailwater depth and the horizontal distance between the impinging jet and the origin of the wall jet. The scour length and the distance between the end of the ridge and the wall jet origin increase with decreasing densimetric Froude number of the impinging jet. The opposite trend occurs for decreasing densimetric Froude number of the wall jet. An empirical relationship for estimating the scour depth due to the simultaneous jet action is given.

**Keywords:** Densimetric Froude number; impinging jet; laboratory experiment; scour; wall jet

## 1 Introduction

The reliable assessment of scour near hydraulic structures is important because excessive scour may cause structural failure. Only few studies have investigated the scour due to double jets, including Uyumaz (1988), Dey and Eldho (2009), and Pagliara *et al.* (2011). Uyumaz (1988) studied scour downstream of a vertical gate with overflow (impinging jet) and underflow (wall jet). The maximum scour depth was found to be smaller for a gate with simultaneous over and underflow. An equation was proposed for estimating the scour depth for two sediments. Simultaneous wall and impinging jets occur if there is flow over and under gates or if low-level outlets and crest spillways operate simultaneously. Then the scour due to combined wall and impinging jets has to be investigated.

## 2 Dimensional analysis

Parameter  $\phi$  represents the scour hole characteristics, including the maximum scour depth  $y_s$ , the scour length  $l_s$ , and the horizontal distance between the ridge end and the wall jet origin  $l_h$  as (Fig. 1)

$$\phi = f(u_w, u_i, D_i, D_w, Y_t, d_{50}, g, \rho_s, \rho, \nu, B, x_p) \quad (1)$$

in which  $u_w$  = wall jet velocity,  $u_i$  = impinging jet velocity,  $D_i$  = impinging jet diameter,  $D_w$  = wall jet diameter,  $Y_t$  = tailwater depth,  $d_{50}$  = median sediment diameter,  $g$  = gravity acceleration,  $\rho_s$  = density of sediment,  $\rho$  = density of water,  $\nu$  = kinematic fluid viscosity,  $B$  = channel width and  $x_p$  = horizontal distance of impinging jet from the wall jet origin. The

Revision received 14 May 2012/Open for discussion until 28 February 2013.

ISSN 0022-1686 print/ISSN 1814-2079 online  
<http://www.tandfonline.com>

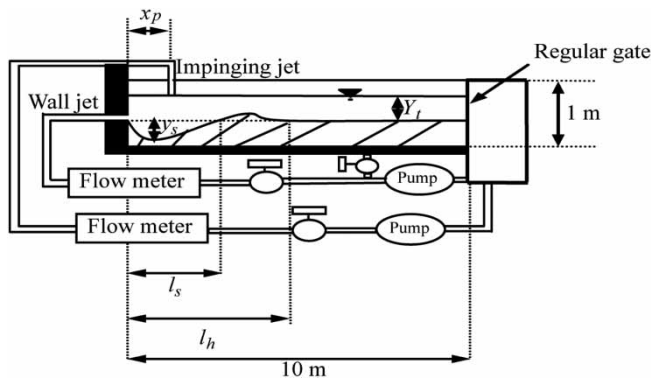


Figure 1 Schematic view of experimental set-up and scour hole parameters

diameters of the two jets were kept equal, i.e.  $D_i = D_w = D$ . Using Buckingham's theorem and neglecting the effect of the jet Reynolds numbers on the scour hole parameters, we obtain

$$\frac{\phi}{D} = f\left(\frac{Y_t}{D}, ER, \frac{x_p}{D}, F_w, F_i\right) \quad (2)$$

in which  $F_w = u_w/[gd_{50}(\rho_s - \rho)/\rho]^{0.5}$  and  $F_i = u_i/[gd_{50}(\rho_s - \rho)/\rho]^{0.5}$  are the densimetric Froude numbers of the wall jet and impinging jet, respectively, and  $ER = B/D$ .

### 3 Experimental set-up and procedure

Experiments were conducted in a 0.58 m wide, 10 m long and 1 m deep channel. Two discharge meters of  $\pm 1.6\%$  accuracy were used. Two pipes of inner diameters of 2 cm and 1 cm were employed for jet creation. Two types of nearly uniform sediment of median sizes  $d_{50} = 0.6$  mm and 1.05 mm with  $\rho_s = 2.65$  t/m<sup>3</sup> were used as bed materials. A sluice gate was located at the channel end to control the tailwater. The tailwater depth and the bed profiles were measured by a digital point gauge of  $\pm 0.01$  mm accuracy. A schematic view of the experimental facilities and the scour hole is shown in Fig. 1. The asymptotic scour time was defined as the time when the scour depth reached its final shape. The latter was found within 24 and 52 h for  $d_{50} = 1.05$  mm and  $d_{50} = 0.6$  mm, respectively.

The maximum scour depth was measured near equilibrium conditions during jet operation (dynamic measurements) and recorded six times using a point gauge. The largest value was considered as the dynamic scour depth (Aderibigbe and Rajaratnam 1996). The maximum scour depth, the scour length, and the horizontal distance of the ridge end from the wall jet origin were also measured after the inflow was stopped and the water drained (static measurements).

By systematically changing  $u_w$ ,  $u_i$ ,  $Y_t$ ,  $D$ ,  $d_{50}$ ,  $x_p$  and  $B$ , a total 120 experiments were conducted with  $F_w$  and  $F_i$  ranging from 9.3 to 25.6,  $x_p/D$  from 5 to 45,  $Y_t/D$  from 3 to 18, and  $ER$  ranging from 5 to 58.

## 4 Results and discussions

### 4.1 Observations

Two main vortices were observed around the impinging jet (Fig. 2(a)), the first occurred in front of the impinging jet, hereafter called front vortex, while the other surrounds the upstream portion of the impinging jet, called scarf vortex (SV). The scour hole can be divided into two portions. The first of the scour hole portion is mainly formed by the wall jet, whereas the impinging jet remains negligible. The second scour hole portion (Fig. 2(b)) is formed by the interaction of the two jets. As the second scour hole portion becomes deeper (Fig. 2(b)), the inner vortex (IN) in the scour hole forms. The difference between the static and dynamic scour measurements was then large. In experiments where the second scour hole portion was shallow, IN vortices were not observed. In plan view, two types of the scour holes were observed. For the first scour hole type (PPT1), the ridge height was maximum at the channel axis and most of the sediment was transported downstream by the wall jet. For the second scour hole type (PPT2), the ridge height was minimum at the channel axis. The SV and the deviation of the wall jet towards the channel side wall are then dominant transporting sediments towards the channel side wall.

In longitudinal direction, two scour hole types may be distinguished. The first LPT1 has one local maximum scour depth  $y_{s1}$ . For the second LPT2, the second scour hole portion is formed by the impinging jet. Observations indicated that by increasing  $F_w$

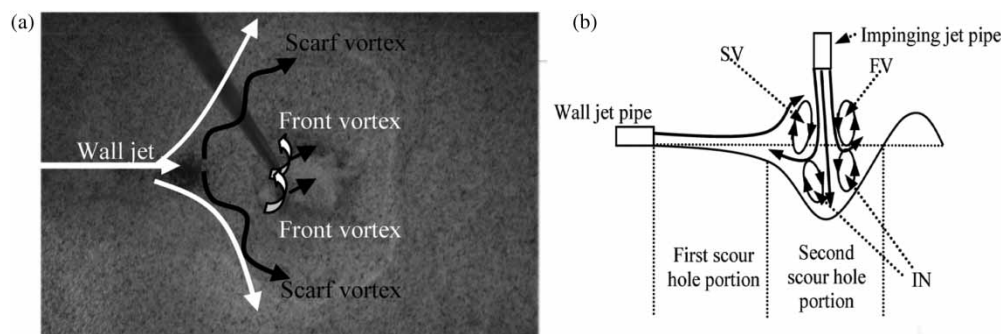


Figure 2 Schematic view of flow in scour hole (a) plan view, (b) longitudinal section

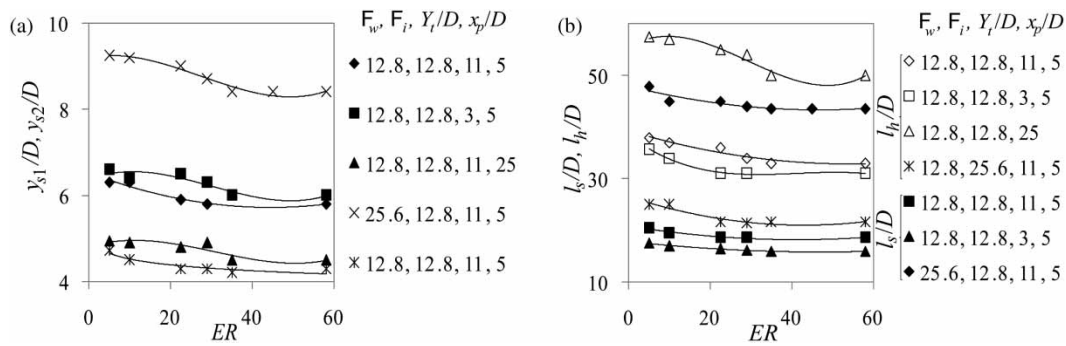


Figure 3 Variation of scour hole parameters with expansion ratio  $ER$  (a)  $y_{s1}/D$  and  $y_{s2}/D$ , (b)  $l_s/D$  and  $l_h/D$

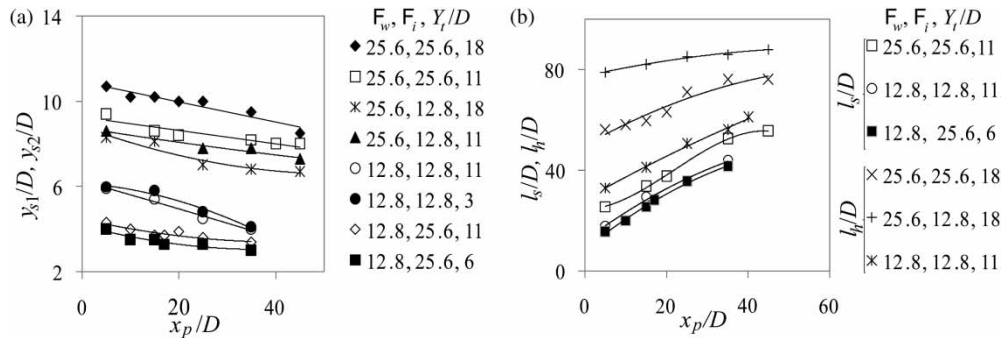


Figure 4 Variation of (a)  $y_{s1}/D$  and  $y_{s2}/D$  with  $x_p/D$ , (b)  $l_s/D$  and  $l_h/D$  with  $x_p/D$

and decreasing  $F_i$ , the probability of occurrence of types PPT2 and LPT2 decreases.

#### 4.2 Effect of non-dimensional scour parameters

Figure 3 shows the effect of the expansion ratio  $ER = B/D$  on  $y_s$ ,  $l_s$  and  $l_h$ . By increasing  $ER$ , these parameters decrease. If the expansion ratio is above a certain value ( $ER_{SV}$ ), its effect can be neglected; according to Lim (1995), this is the case for  $ER > 5$  for the single wall jet, whereas Sui *et al.* (2008) state  $ER > 31$ . In this study, for  $F_w = F_i = 12.8$ ,  $Y_t/D = 11$ , and  $x_p/D = 5$ , a value of  $ER_{SV} = 22.5$  applies, whereas for  $F_w = F_i = 12.8$ ,  $Y_t/D = 3$  and  $x_p/D = 5$  a value of  $ER_{SV} = 35$  was obtained. By decreasing the tailwater depth, the effect of the expansion ratio on the scour increases. By increasing  $x_p/D$  from 5 to 25,  $ER_{SV}$  increases from 22.5 to 35. By increasing  $F_w$  from 12.8 to 25.6,  $ER_{SV}$  increases also from 22.5 to 35, whereas  $F_i$  has no significant effect on  $ER_{SV}$ . The effect of the expansion ratio on the scour depends also on the range of the other non-dimensional parameters, explaining the differences between Lim (1995) and Sui *et al.* (2008).

Ali and Lim (1986), Lim (1995), Aderibigbe and Rajaratnam (1996), Sarathi *et al.* (2008), and Sui *et al.* (2008) demonstrated that the scour depth and length increase with the densimetric Froude number. Figure 3(a) confirms this trend for the scour depth due to the two jets. From Fig. 3(b) it is evident that the relative scour hole lengths  $l_s/D$  and  $l_h/D$  decrease with increasing  $F_i$  but increase with increasing  $F_w$ . This trend for the single wall jet is in line with Ali and Lim (1986) and Sarathi *et al.* (2008), but not for the scour due to single impinging jet made by

Aderibigbe and Rajaratnam (1996). The impinging jet behaves like an obstacle for the development of the wall jet. Thus by increasing  $F_i$ , the wall jet deviates more towards the channel side wall. As a consequence, the scour lengths  $l_s/D$  and  $l_h/D$  decrease.

Figure 4(a) shows the effect of the impinging jet distance from the wall jet origin on the scour depth. The maximum scour depths  $y_{s1}/D$  and  $y_{s2}/D$  decrease with increasing  $x_p/D$ . Figure 4(b) reveals that the scour length  $l_s/D$  and  $l_h/D$  increase with increasing  $x_p/D$ . If the impinging jet is located near the wall jet origin, both jets contribute to the scour development. By increasing  $x_p/D$ , the wall jet diffuses in the longitudinal direction so that  $y_{s1}/D$  and  $y_{s2}/D$  decrease.

The effect of the tailwater depth ratio on  $y_{s1}/D$ ,  $y_{s2}/D$ ,  $l_s/D$  and  $l_h/D$  due to simultaneous wall jet and impinging jet is shown in Fig. (5). Because of suspended sediment presence in the scour hole, the scour depth differed for static and dynamic measurements. For the static measurements, the scour depth increases with the tailwater depth ratio, whereas for dynamic measurements the scour depth decreases, as observed by Aderibigbe and Rajaratnam (1996) for scour due to an impinging jet. For identical data in static and dynamic measurements, the scour depth decreases with increase in the tailwater depth ratio.

The scour lengths  $l_s/D$  and  $l_h/D$  increase with the tailwater depth ratio. Because of impinging jet diffusion in the tailwater, the wall jet develops more in the longitudinal direction for high tailwater, so that these two scour lengths are more pronounced for high tailwater.

According to dimensional analysis as in Eq. (2), the scour depth can be expressed with coefficient  $A$  and  $F$ , and the

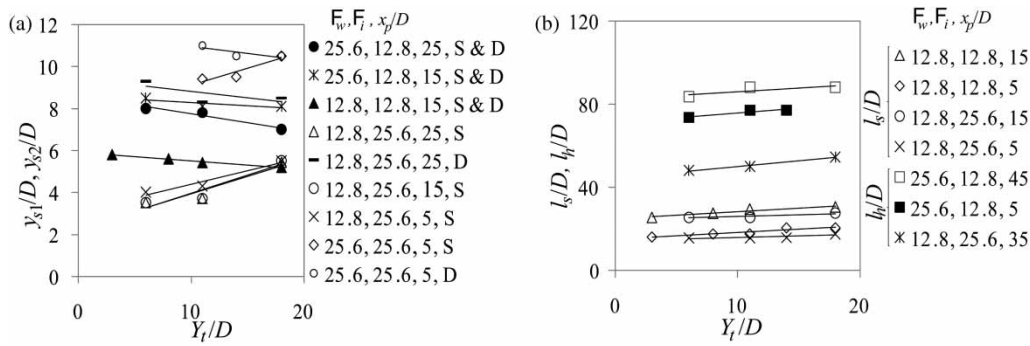


Figure 5 (a) Variation of  $y_{s1}/D$  and  $y_{s2}/D$  with  $Y_t/D$ , (b)  $l_s/D$  and  $l_h/D$  with  $Y_t/D$ . S (static), D (dynamic) measurement

exponents  $B, C, E, H$  and  $I$  as empirical constants as

$$\frac{y_s}{D} = A(F_w)^B (F_i)^C \left(\frac{Y_t}{D}\right)^E \left(F + \ln\left(\frac{B}{D}\right)\right)^H \left(\frac{x_p}{D}\right)^I \quad (3)$$

Different equations were examined and Eq. (3) resulted as the best fit. To test the effect of each of non-dimensional parameter on the scour, the parameters on the right-hand side of Eq. (3) were omitted one by one to obtain the empirical constants. By omitting  $Y_t/D$ ,  $F_w$ ,  $F_i$  and  $x_p/D$ , the accuracy of the equations decreases significantly, whereas by omitting  $B/D$ , no significant change was observed. This means that the expansion ratio has a secondary effect on the scour hole depth. Based on the experimental data, the following equation was derived for  $Y_s/D$ :

$$\frac{y_s}{D} = 0.478(F_w)^{0.54} (F_i)^{0.54} \left(\frac{Y_t}{D}\right)^{-0.034} \left(\frac{x_p}{D}\right)^{-0.1}, \quad R^2 = 0.8 \quad (4)$$

Equation (4) approximates the scour depth due to simultaneous wall jet and impinging jet of identical size if  $9.3 < F_w, F_i < 25.6$ ,  $3 < Y_t/D < 18$ ,  $5 < x_p/D < 45$  and  $5 < ER < 58$ .

## 5 Conclusions

The scour hole parameters due to simultaneous wall and impinging jets were investigated systematically. By increasing the expansion ratio, the scour hole parameters decrease. For expansion ratios above a specific value, its effect on the scour hole parameters is small. This limit value is higher for small tailwater depth, high densimetric Froude number of the wall jet and longer horizontal distance between the impinging jet and the wall jet origin.

Increasing the densimetric Froude number of the jet, the scour depth increases for dynamic measurements. Under static conditions, the scour depth increases with the densimetric Froude number of the wall jet, but decreases with the densimetric Froude number of the impinging jet. The scour length and the horizontal distance between the ridge end and the wall jet origin increase with the tailwater depth ratio. For a longer distance between the

impinging jet and the wall jet origin, the wall jet diffuses more so that the scour depth decreases. Furthermore, the scour length and the horizontal distance between the ridge end and the wall jet origin increase.

A sensitivity analysis indicates that the expansion ratio has a secondary effect on the scour hole parameters as compared with other non-dimensional parameters. An empirical equation for the scour depth is presented.

## Notation

$B$	= channel width (m)
$D$	= pipe diameter (m)
$d_{50}$	= mean bed material diameter (m)
$ER$	= jet expansion ratio (—)
$ER_{SV}$	= limit expansion ratio (—)
$F_i$	= densimetric Froude number of impinging jet (—)
$F_w$	= densimetric Froude number of wall jet (—)
$g$	= gravity acceleration ( $\text{m/s}^2$ )
$Y_t$	= tailwater depth (m)
$l_s$	= scour length (m)
$l_h$	= horizontal distance between ridge end and wall jet (m)
$u_i$	= impinging jet velocity (m/s)
$u_w$	= wall jet velocity (m/s)
$x_p$	= horizontal distance of impinging jet from wall jet (m)
$y_s$	= scour depth (m)
$\nu$	= kinematic viscosity of water ( $\text{m}^2/\text{s}$ )
$\rho$	= density of water ( $\text{kg/m}^3$ )
$\rho_s$	= density of sediment ( $\text{kg/m}^3$ )
$\phi$	= scour hole characteristic (m)

## References

- Aderibigbe, O., Rajaratnam, N. (1996). Erosion of loose beds by submerged circular impinging vertical turbulent jets. *J. Hydraulic Res.* 34(1), 19–33.
- Ali, K.H.M., Lim, S.Y. (1986). Local scour caused by submerged wall jets. *Proc. Inst. Civil Eng.* 81(2), 607–645.
- Dey, D., Eldho, T.I. (2009). Effect of spacing of two off-set jets on scouring phenomena. *J. Hydraulic Res.* 47(1), 82–89.

- Lim, S.Y. (1995). Scour below un-submerged full flowing culvert outlets. *Proc. Inst. Civil Eng.* 112(2), 136–149.
- Pagliara, S., Palermo, M., Carnacina, L. (2011). Scour process due to symmetric dam spillways crossing jets. *Int. J. River Basin Manage.* 9(1), 31–42.
- Sarathi, P., Faruque, M.A.A., Balachandar, R. (2008). Influence of tailwater depth sediment size and densimetric Froude number on scour by submerged square wall jets. *J. Hydraulic Res.* 46(2), 158–175.
- Sui, J., Faruque, M.A.A., Balachandar, R. (2008). Influence of channel width and tailwater depth on local scour caused by square jets. *J. Hydro-Environment Res.* 2(1), 39–45.
- Uyumaz, A. (1988). Scour downstream of the vertical gate. *J. Hydraulic Eng.* 114(7), 811–816.